Title: Sperm membrane proteins DCST1 and DCST2 are required for the sperm-egg fusion process in mice and fish

Authors: Taichi Noda[1,2], Andreas Blaha[3,4], Yoshitaka Fujihara[1,5], Krista R. Gert[3,4], Chihiro Emori[1], Victoria E. Deneke[3], Seiya Oura[1,6], Sara Berent[3], Mayo Kodani[1,6], Karin Panser[3], Luis Enrique Cabrera-Quio[3,4], Andrea Pauli[3,*], Masahito Ikawa[1,6,7,*]

Affiliation:

[1]Research Institute for Microbial Diseases, Osaka University, 3-1 Yamadaoka, Suita, Osaka 565-0871, Japan

[2]Institute of Resource Development and Analysis, Kumamoto University, 2-2-1 Honjo, Kumamoto 860-0811, Japan

[3]Research Institute of Molecular Pathology (IMP), Vienna BioCenter (VBC), Campus-Vienna-Biocenter 1, 1030 Vienna, Austria

[4]Vienna BioCenter PhD Program, Doctoral School of the University at Vienna and Medical University of Vienna, Vienna, Austria

[5]Department of Bioscience and Genetics, National Cerebral and Cardiovascular Center, Suita, Osaka 564-8565, Japan

[6]Graduate School of Pharmaceutical Sciences, Osaka University, 1-6 Yamadaoka, Suita, Osaka 565-0871, Japan

[7]The Institute of Medical Science, The University of Tokyo, 4-6-1 Shirokanedai, Minato-ku, Tokyo 108-8639, Japan

*Correspondences and requests for materials should be addressed to A.P. (email: andrea.pauli@imp.ac.at) and M.I. (email: ikawa@biken.osaka-u.ac.jp).

Abstract

The process of sperm-egg fusion is critical for successful fertilization, yet the underpinning mechanisms that regulate these steps have remained unclear in vertebrates. Here, we show that both mouse and zebrafish DCST1 and DCST2 are necessary in sperm to fertilize the egg, similar to their orthologs SPE-42 and SPE-49 in *C. elegans* and Sneaky in *D. melanogaster*. Mouse *Dcst1* and *Dcst2* single knockout (KO) spermatozoa are able to undergo the acrosome reaction and show normal relocalization of IZUMO1, an essential factor for sperm-egg fusion, to the equatorial segment. While both single KO spermatozoa can bind to the oolemma, they rarely fuse with oocytes, resulting in male sterility. Similar to mice, zebrafish *dcst1* KO males are subfertile and *dcst2* and *dcst1/2* double KO males are sterile. Zebrafish *dcst1/2* KO spermatozoa are motile and can approach the egg, but rarely bind to the oolemma. These data demonstrate that DCST1/2 are essential for male fertility in two vertebrate species highlighting their crucial role as conserved factors in fertilization.

Main text

Introduction

Until recently, only a few factors had been shown to be essential for the sperm-egg fusion process: IZUMO1 on the sperm membrane and its receptor (IZUMO1R, also known as JUNO and FOLR4) on the egg membrane (oolemma)[1,2]. Mammalian IZUMO1 and JUNO form a 1:1 complex, which is necessary for sperm-egg adhesion prior to fusion[1,3,4]. Furthermore, egg-expressed CD9 is also required for sperm-egg fusion, yet its role appears to be indirect by regulating microvilli formation on the oolemma rather than fusion[5-8]. Recently, we and other research groups have found that four additional sperm factors [fertilization influencing membrane protein (FIMP), sperm-oocyte fusion required 1 (SOF1), transmembrane protein 95 (TMEM95), and sperm acrosome associated 6 (SPACA6)] are also essential for the sperm-egg fusion process and male fertility in mice[9-12]. However, HEK293 cells expressing all of these sperm-expressed, fusion-related factors in addition to IZUMO1 were able to bind but not fuse with zona pellucida (ZP)-free eggs, suggesting that additional fusion-related factors are necessary for the completion of sperm-egg fusion[11].

DCSTAMP and OCSTAMP proteins represent an interesting group of proteins to study in the context of cell-cell fusion, since they have been shown to play a role in osteoclast and foreign body giant cell (FBGC) fusion[13-15]. They belong to the class of DC-STAMP-like domain-containing proteins, and are multi-pass transmembrane proteins with an intracellular C-terminus containing a non-canonical RING finger domain[13,16,17]. DCSTAMP was shown to localize to the plasma membrane and endoplasmic reticulum (ER) membrane in dendritic cells and osteoclasts[16-19]. These cell types in *Dcstamp* KO mice show no apparent defect in differentiation into the osteoclast lineage and cytoskeletal structure, yet osteoclasts and FBGCs are unable to fuse to form terminally differentiated multinucleated cells[14]. Even though OCSTAMP is widely expressed in mouse tissues[20], the only reported defect in *Ocstamp* KO mice is the inability to form multinucleated osteoclasts and FBGCs[13,15]. The fusion defect is not due to a change in the expression levels of osteoclast markers, including *Dcstamp*[13,15]. These results established an essential role for DC-STAMP-like domain-containing proteins in cell-cell fusion.

DC-STAMP-like domain-containing proteins, namely the testis-enriched SNKY, SPE-42, and SPE-49, are necessary for male fertility in *Drosophila*[21,22] and *C. elegans*[23-25], respectively. Specifically, *sneaky*-disrupted fly spermatozoa can enter the egg, but fail to break down the sperm plasma membrane: the male pronucleus thus does not form, and embryonic mitotic divisions do not occur[22]. *Spe-42* and *spe-49* mutant *C. elegans* spermatozoa can migrate into the spermatheca, the site of fertilization in worms, but these mutants are nearly or completely sterile, respectively, suggesting that SPE-42 and SPE-49 are involved in the ability of spermatozoa to fertilize eggs[23-25]. SNKY, SPE-42 and SPE-49 have homologs in vertebrates called DCST1 and DCST2, but the roles of these proteins have remained undetermined. Here, we analyzed the physiological function of *Dcst1* and *Dcst2* and their effect on sperm fertility using genetically modified mice and zebrafish.

Results

DCST1 and DCST2 are required for male fertility in mice.

RT-PCR analysis with multiple mouse tissues showed that *Dcst1* and *Dcst2* mRNAs are abundantly expressed in mouse testis (**Figure 1A**). Using published single-cell RNA-sequencing data[26], we found that *Dcst1* and *Dcst2* mRNAs peak in mid-round spermatids, indicating that the expression patterns of *Dcst1* and *Dcst2* are similar to that of the other sperm-egg fusion-related genes *Izumo1*, *Fimp*, *Sof1*, *Tmem95*, and *Spaca6* (**Figure 1B**). DCST1 and DCST2 are conserved in vertebrates from fish to humans (**Figure S1A**). Sequence homology between mouse DCST1 and mouse DCST2 was 24.3% at the amino acid level using Clustal Omega (**Figure S1B**). DCST1 and DCST2 have multiple (six to eight) predicted transmembrane (TM) helices (**Figure S1C**), and an atypical C_4C_4 RING finger domain at their intracellular C-termini that is required for SPE-42 function in *C. elegans*[25].

Using CRISPR/Cas9-mediated mutagenesis, we generated *Dcst2* mutant mice lacking 7,223 bp ($Dcst2^{del/del}$), which resulted in the deletion of almost all of the *Dcst2* open reading frame (ORF) (**Figure S2A-C**). Of note, the expression level of *Dcst1* mRNA in $Dcst2^{del/del}$ testis decreased (**Figure S2D**), suggesting that the deleted region is required for *Dcst1* expression in the testis. As shown in **Figure S2A**, *Dcst1* and *Dcst2* are tandemly arranged such that parts of their 5' genomic regions overlap. To assess the role of each gene, we generated *Dcst1* indel mice ($Dcst1^{d1/d1}$) and *Dcst2* indel mice ($Dcst2^{d25/d25}$) (**Figure S3A and B**). RNA isolation from mutant testes followed by cDNA sequencing revealed that $Dcst1^{d1/d1}$ has a 1-bp deletion in exon 1, and $Dcst2^{d25/d25}$ has a 25-bp deletion in exon 4 (**Figure S3C and D**). Both deletions result in frameshift mutations leading to premature stop codons.

The $Dcst1^{d1/d1}$, $Dcst2^{d25/d25}$, and $Dcst2^{del/del}$ male mice successfully mated with female mice, but the females rarely delivered offspring {pups/plug: 9.01 ± 2.77 [control (Ctrl), 19 plugs], 0.22 ± 0.19 [$Dcst1^{d1/d1}$, 17 plugs], 0 [$Dcst2^{d25/d25}$, 42 plugs], 0 [$Dcst2^{del/del}$, 24 plugs]}, indicating that these males are almost sterile (**Figure 1C**). Unexpectedly, the indel mutations in $Dcst1^{d1/d1}$ and $Dcst2^{d25/d25}$ decreased the expression level of *Dcst1* mRNA in $Dcst2^{d25/d25}$ testis and *Dcst2* mRNA in $Dcst1^{d1/d1}$ testis, respectively (**Figure S3C**). To evaluate the influence of the decreased expression level of *Dcst1* and *Dcst2* mRNAs on male fertility, we obtained double heterozygous ($Dcst1^{d1/wt}$ and $Dcst2^{del/wt}$) (dHZ) males through intercrossing. The dHZ males showed a decreased expression level of both *Dcst1* and *Dcst2* mRNA in the testis, but their fertility was comparable to that of the control (**Figure S3E**), indicating that the expression levels of *Dcst1* mRNA from the $Dcst2^{d25}$ allele and *Dcst2* mRNA from the $Dcst1^{d1}$ allele are decreased but still sufficient to maintain male fertility. This data reconfirms that DCST2 is indispensable for male fertility. Hereafter, we used $Dcst1^{d1/d1}$ and $Dcst2^{d25/d25}$ male mice for all experiments unless otherwise specified.

Spermatozoa from $Dcst1^{d1/d1}$ and $Dcst2^{d25/d25}$ mice rarely fertilize eggs.

The gross morphology of $Dcst1^{d1/d1}$ and $Dcst2^{d25/d25}$ testes was comparable to the control (**Figure S4A**). Although the testis weight of $Dcst1^{d1/d1}$ was slightly reduced [testis weight (mg)/body weight (g): 3.13 ± 0.19 ($Dcst1^{d1/wt}$), 2.56 ± 0.27 ($Dcst1^{d1/d1}$), 3.88 ± 0.34 ($Dcst2^{d25/wt}$), 3.60 ± 0.28 ($Dcst2^{d25/d25}$)] (**Figure S4B**), PAS-hematoxylin

staining revealed no overt defects in spermatogenesis of *Dcst1*$^{d1/d1}$ and *Dcst2*$^{d25/d25}$ males (**Figure S4C**). The sperm morphology and motility parameters of *Dcst1*$^{d1/d1}$ and *Dcst2*$^{d25/d25}$ mice were normal (**Figure S5**). However, when the mutant spermatozoa were incubated with cumulus-intact wild-type (wt) eggs *in vitro*, they accumulated in the perivitelline space and could not fertilize eggs [96.5 ± 7.1% (Ctrl, 231 eggs), 0% (*Dcst1*$^{d1/d1}$, 97 eggs), and 0% (*Dcst2*$^{d25/d25}$, 197 eggs)] (**Figure 1D-E and Movies S1-2**). Furthermore, even when these KO spermatozoa were incubated with ZP-free eggs, only one egg and no eggs were fertilized with *Dcst1* KO spermatozoa and *Dcst2* KO spermatozoa, respectively [100% (Ctrl, 142 eggs), 0.8 ± 1.6% (*Dcst1*$^{d1/d1}$, 94 eggs), 0% (*Dcst2*$^{d25/d25}$, 88 eggs)] (**Figure 1F**).

Spermatozoa from *Dcst1*$^{d1/d1}$ and *Dcst2*$^{d25/d25}$ mice can bind to, but not fuse with eggs.

To examine the binding and fusion ability of *Dcst1*$^{d1/d1}$ and *Dcst2*$^{d25/d25}$ mutant spermatozoa, we incubated these mutant spermatozoa with zona pellucida (ZP)-free eggs. Both mutant spermatozoa could bind to the oolemma [5.72 ± 1.97 (Ctrl, 113 eggs), 7.64 ± 4.68 (*Dcst1*$^{d1/d1}$, 89 eggs), 7.63 ± 3.45 (*Dcst2*$^{d25/d25}$, 89 eggs)] (**Figure 2A and B**). Because binding is not defective in mutant spermatozoa, we confirmed that IZUMO1, a key factor in this process, was expressed and localized normally in testicular germ cells (TGC) and spermatozoa of *Dcst1*$^{d1/d1}$ and *Dcst2*$^{d25/d25}$ males (**Figure 2C**). Indeed, we found that the level of IZUMO1 in mutant spermatozoa was comparable to the control (**Figure 2C**). Moreover, there was no difference in the acrosome reaction rate of oolemma-bound spermatozoa between control, *Dcst1*$^{d1/d1}$ and *Dcst2*$^{d25/d25}$ males, determined by live-cell staining with IZUMO1 antibody [58.9 ± 17.9% (Ctrl), 80.5 ± 4.6% (*Dcst1*$^{d1/d1}$), 63.5± 6.5% (*Dcst2*$^{d25/d25}$)] (**Figure 2D and E**). Next, the mutant spermatozoa were incubated with Hoechst 33342-preloaded ZP-free eggs. In experiments with control spermatozoa, Hoechst 33342 fluorescence signal was translocated into sperm heads (**Figure 2F**), indicating that these spermatozoa fused with the egg membrane. However, Hoechst 33342 signal was rarely detected in *Dcst1* KO and *Dcst2* KO spermatozoa bound to the oolemma [fused spermatozoa/egg: 1.52 ± 0.35 (Ctrl, 113 eggs), 0.04 ± 0.05 (*Dcst1*$^{d1/d1}$, 73 eggs), 0 (*Dcst2*$^{d25/d25}$, 73 eggs)] (**Figure 2F and G**). Thus, *Dcst1* and *Dcst2* KO spermatozoa can bind to eggs but not fuse with them.

Sterility of *Dcst1*$^{d1/d1}$ and *Dcst2*$^{d25/d25}$ males is rescued by *Dcst1*-3xHA and *Dcst2*-3xHA transgenes.

To confirm that the *Dcst1* and *Dcst2* disruptions are responsible for male sterility, we generated transgenic mice in which a testis-specific Calmegin (*Clgn*) promoter expresses mouse DCST1 and DCST2 with a HA tag at the C-terminus (**Figure S6A and B**). When *Dcst1*$^{d1/d1}$ males with the *Dcst1*-3xHA transgene and *Dcst2*$^{d25/d25}$ males with the *Dcst2*-3xHA transgene were mated with *wt/wt* females, the females delivered normal numbers of offspring [pups/plug: 5.7 ± 0.5 (*Dcst1*$^{d1/d1}$; Tg, 25 plugs), 7.6 ± 2.7 (*Dcst2*$^{d25/d25}$; Tg, 15 plugs)] (**Figure 3A**). We could detect HA-tagged DCST1 and HA-tagged DCST2 in TGCs and spermatozoa at the expected sizes for the full-length proteins (**Figure 3B**, arrowheads), though both proteins appear to be subject to post-translational processing/protein degradation.

To reveal the localization of DCST1 and DCST2 in spermatozoa, we performed immunocytochemistry with an antibody detecting the HA epitope and peanut agglutinin (PNA) as a marker for the sperm acrosome reaction. As shown in **Figure 3C**, PNA in the anterior acrosome was translocated to the equatorial segment after the acrosome reaction as shown previously[27]. While HA-tagged DCST1 could rarely be observed in spermatozoa, HA-tagged DCST2 was detected within the anterior acrosome of acrosome-intact spermatozoa, and then translocated to the equatorial segment after the acrosome reaction (**Figure 3C**), mirroring the relocalization of IZUMO1 upon the acrosome reaction[28]. The fluorescence in the sperm tail was observed in both control and *Dcst2-HA* Tg spermatozoa, indicating that the signal in the tail was non-specific (**Figure 3C**).

Taking advantage of the HA tag, we obtained co-immunoprecipitation (co-IP) samples. While HA-tagged DCST1 was detected only in TGCs, HA-tagged DCST2 was detected in both TGCs and spermatozoa (**Figure 3D**). We could not detect IZUMO1 in these IP samples (**Figure 3D**), suggesting that DCST1 and DCST2 do not form a complex with IZUMO1. Since both DCSTs are tagged with HA, we could not examine their interaction *in vivo*. Instead, we could confirm the presence of the DCST1/DCST2 complex when we expressed *Dcst1*-3xFLAG and *Dcst2*-3xHA in HEK293T cells (**Figure 3E**).

HEK293T cells expressing DCST1/2 and IZUMO1 bind to but do not fuse with ZP-free eggs.

To assess whether DCST1 and DCST2 are sufficient for inducing sperm-egg fusion, we overexpressed *Dcst1*-3xFLAG, *Dcst2*-3xHA, and *Izumo1*-1D4 in HEK293T cells (**Figure 4A**). HEK293T cells overexpressing IZUMO1 could bind to, but not fuse with, ZP-free eggs (**Figure 4B**), which was consistent with previous reports[4,11]. In contrast, HEK293T cells overexpressing DCST1 and DCST2 failed to bind to ZP-free eggs (**Figure 4B and C**). Co-expression of IZUMO1 and DCST1/2 allowed the cells to bind to ZP-free eggs [4.24 ± 2.41 cells/eggs (IZUMO1), 2.01 ± 1.93 cells/eggs (DCST1/2 + IZUMO1)], but did not facilitate fusion with the oolemma (**Figure 4B and C**). Thus, though DCST1 and DCST2 appear to have a role in the sperm-egg fusion process, they are not sufficient to induce fusion, even in conjunction with IZUMO1.

Sperm-expressed Dcst1/2 are also required for fertilization in zebrafish.

DCST1/2 are widely conserved and expressed in the male germ line of many metazoans, which is remarkable for the otherwise rapidly evolving group of sperm-egg interacting proteins[29,30]. To assess to what extent our findings in mice could be expanded among vertebrate species, we asked what the roles of DCST1/2 are in an evolutionarily distant vertebrate species, the zebrafish. The orthologous zebrafish genes *dcst1* and *dcst2* are expressed specifically in testis and arranged similarly to mouse *Dcst1/2* (**Figure S7A and B**). We therefore generated three independent KO fish lines, *dcst1* (*dcst1*$^{-/-}$), *dcst2* (*dcst2*$^{-/-}$), or both (*dcst1/2*$^{-/-}$), by CRISPR/Cas9-mediated mutagenesis (**Figure S7B and C**).

Lack of zebrafish Dcst2 alone or in combination with Dcst1 caused complete sterility in males, whereas lack of Dcst1 alone led to severe subfertility [5.5 ± 3.6% fertilization rate (*dcst1*$^{-/-}$, 16 clutches)] (**Figure 5A**). The fertility of heterozygous males and KO

females, however, was comparable to the *wt/wt* control males. (**Figure 5A**). Thus, similar to mice, Dcst1/2 are essential for male fertility in zebrafish. For further phenotypic analyses we decided to focus on the *dcst2*$^{-/-}$ mutant (unless stated otherwise), since loss of Dcst2 is sufficient to cause complete sterility.

To understand what causes the fertility defect, we determined whether spermatozoa were produced in mutant males and where Dcst proteins were localized in *wt/wt* males. *Dcst1*$^{-/-}$ and *dcst2*$^{-/-}$ males showed normal mating behavior and produced morphologically normal spermatozoa, indicating that zebrafish Dcst1/2 are not crucial for spermatogenesis (**Figure 5B**). Because zebrafish sperm lack an acrosome, we examined the localization of Dcst2. To this end, we produced antibodies against the C-terminal RING finger domain of zebrafish Dcst2. Dcst2 antibodies could detect zebrafish Dcst2 protein as determined by western blotting of wt and *dcst2*$^{-/-}$ sperm lysates (**Figure S7D**) and immunofluorescence staining of Dcst2-superfolder GFP (sfGFP) overexpression in the zebrafish embryo (**Figure S7E**). Interestingly, immunofluorescence against Dcst2 strongly stained wt spermatozoa at the periphery of the head in punctae and occasionally the mid-piece (**Figure 5C**). Weaker staining of the tail region was also detected in *dcst2*$^{-/-}$ spermatozoa, suggesting that this signal was unrelated to Dcst2. Thus, Dcst2 localizes to the plasma membrane of the sperm head.

When added to wt eggs, *dcst2*$^{-/-}$ spermatozoa were able to locate and enter the micropyle, the funnel-shaped site of sperm entry (**Figure 5D**), but most of the entering mutant spermatozoa were expelled from the micropyle shortly thereafter. We therefore conclude that Dcst2 is neither required for overall sperm motility nor for spermatozoa to approach and enter the micropyle. After entering the micropyle, wt zebrafish spermatozoa immediately bind to the oolemma. We previously established an assay to assess sperm-egg binding during zebrafish fertilization[31]. Building on this assay, we used live imaging of spermatozoa and eggs to quantify the number of sperm adhered to the oolemma within a physiologically relevant time frame [1.97 ± 0.97 spermatozoa/100 µm (12 eggs)] (**Figure 5E and F**). Employing this assay with *dcst2*$^{-/-}$ spermatozoa revealed that *dcst2*$^{-/-}$ spermatozoa are unable to adhere to wt eggs stably [0.05 ± 0.1 spermatozoa/100 µm (9 eggs)] (**Figure 5E and F**). We therefore conclude that zebrafish Dcst2 is required for stable binding of spermatozoa to the oolemma.

Discussion

We demonstrated that the testis-enriched proteins DCST1/2 are necessary for male fertility in mice and fish. These results correspond with similar studies found in *Drosophila* Sneaky and *C. elegans* SPE-42/49 mutants, indicating that the physiological function of DCST1/2 is widely conserved among species. Beside DCST1/2, mammals have DCSTAMP/OCSTAMP, but phylogenetic analysis (**Figure S8A**), mRNA expression pattern (**Figure S8B**), and amino acid homology rate (**Figure S8C**) support their divergence in physiological functions during evolution.

Similar to a previous study suggesting that OCSTAMP and DCSTAMP form a dimer or oligomer on the cell surface as part of a receptor complex[32], our study revealed that DCST1 and DCST2 interact when overexpressed in somatic cells (**Figure 3E**),

implying the formation of a stable DCST1/2 complex on the sperm membrane. We detected mouse DCST2 at the equatorial segment of acrosome-reacted spermatozoa and zebrafish Dcst2 at the periphery of the sperm head. Given that DCST1/2 are TM proteins, these localization patterns suggest that part of the protein is exposed on the sperm surface. We therefore speculate that DCST1/2 either helps organize the fusion-competent sperm membrane or directly interacts with other binding- and/or fusion-relevant molecules on the oolemma. To test this hypothesis, we overexpressed DCST1 and DCST2 in IZUMO1-expressing HEK293T cells. These cells could bind to but not fuse with ZP-free eggs (**Figure 4B-C**), which could be due to lack of other sperm-oocyte fusion-related factors (FIMP, SOF1, TMEM95, and SPACA6). It is difficult to stably express all sperm fusion-related factors (DCST1/2, IZUMO1, FIMP, SOF1, TMEM95, and SPACA6) in culture cells as we have shown in **Figure 4A**. Future investigations need to optimize the experimental conditions of gamete fusion using culture cells and ZP-free eggs.

The function of DCST1/2 in the sperm-egg fusion process differs between mice and fish: mouse DCST1/2 are required for the fusion process after sperm-egg binding (**Figure 2**), and zebrafish Dcst1/2 are required for the sperm-egg binding (**Figure 5**). Fertilization-related factors are known to be among the most rapidly evolving proteins[29,30]. Given the intrinsic diversity of the fertilization process across the animal kingdom, it may be that while DCST proteins are highly conserved, they may have evolved different roles to fit into the specific context of fertilization for a given species or animal group. As we presented here, application of the CRISPR/Cas9-mediated KO screening in a wide variety of animals will shed light on the fundamental mechanism of fertilization and its diversification during evolution.

Materials and Methods

Animals.

B6D2F1, C57BL/6J, and ICR mice were purchased from Japan SLC and CLEA Japan. Mice were acclimated to 12-h-light/12-h-dark cycle. All animal experiments were approved by the Animal Care and Use Committee of the Research Institute for Microbial Diseases, Osaka University, Japan (#Biken-AP-H30-01).

Zebrafish (*Danio rerio*) were raised according to standard protocols (28°C water temperature; 14/10-hour light/dark cycle). TLAB zebrafish served as *wt/wt* zebrafish for all experiments, and were generated by crossing zebrafish AB stocks with natural variant TL (Tüpfel longfin) stocks. *Dcst1*$^{-/-}$, *dcst2*$^{-/-}$, and *dcst1/2*$^{-/-}$ mutant zebrafish were generated as part of this study as described in detail below. All fish experiments were conducted according to Austrian and European guidelines for animal research and approved by the local Austrian authorities (animal protocol GZ: 342445/2016/12).

Mouse sample collection.

Multi-tissue expression analyses were conducted as described previously[11]. For western blotting, TGC proteins were extracted with Pierce IP lysis buffer (Thermo Fisher Scientific) (**Figure 3B and D**) or RIPA buffer [50 mM Tris HCl, 0.15 M NaCl, 1% Sodium deoxycholate, 0.1% SDS, 1% (vol/vol) TritonX-100, pH 7.5] containing a 1% (vol/vol) protease inhibitor mixture (Nacalai Tesque) (**Figure 2C**). Proteins of cauda epididymal spermatozoa were extracted with Pierce IP lysis buffer containing a 1% (vol/vol) protease inhibitor mixture (**Figure 3D**) or SDS sample buffer containing β-mercaptoethanol (Nacalai Tesque) (**Figures 2C and 3B**) as described previously[33].

RT-PCR for mouse multi-tissue expression analyses.

Total RNA was reverse-transcribed into cDNA using a SuperScript III First-Strand Synthesis System for RT-PCR (Invitrogen). PCR was conducted with primer sets (**Table S1**) and KOD-Fx neo (TOYOBO). The PCR conditions were initial denaturation at 94°C for 3 minutes, denaturing at 94°C for 30 seconds, annealing at 65°C for 30 seconds, and elongation at 72°C for 30 seconds for 30 or 35 cycles in total, followed by 72°C for 2 minutes.

Single cell RNA-seq (scRNAseq) analysis.

The Median-Normalized average of *Dcst1*, *Dcst2* and fusion-related genes (*Fimp*, *Izumo1*, *Sof1*, *Spaca6*, and *Tmem95*) in spermatogenesis was examined in the published scRNAseq database[26].

Mouse mating test.

KO male mice were caged with two B6D2F1 females for more than 1 month. After the mating period, male mice were removed from the cages, and the females were kept for another 20 days to allow them to deliver offspring. Frozen spermatozoa from *Dcst1*$^{d1/wt}$ males [B6D2-Dcst1<em2Osb> RBRC#10332, CARD#2702] and *Dcst2*$^{d25/wt}$ males [B6D2-Dcst2<em2Osb> Tg(CAG/Su9-DsRed2,Acr3-EGFP)RBGS002Osb, RBRC#11243, CARD#3047] will be available through RIKEN BRC (http://en.brc.riken.jp/index.shtml) and CARD R-BASE (http://cardb.cc.kumamoto-u.ac.jp/transgenic/).

Mouse sperm motility and *in vitro* fertilization.

Cauda epididymal spermatozoa were squeezed out and dispersed in PBS (for sperm morphology) and TYH (for sperm motility and IVF)[34]. After incubation of 10 and 120 minutes in TYH, sperm motility patterns were examined using the CEROS II sperm analysis system[35-37]. IVF was conducted as described previously[38]. Protein extracts from the remaining sperm suspension in PBS and TYH drops were used for co-IP experiments.

Antibodies.

Rat monoclonal antibodies against mouse IZUMO1 (KS64-125) and mouse SLC2A3 (KS64-10) were generated by our laboratory as described previously[39,40]. The mouse monoclonal antibody against 1D4-tag was generated using a hybridoma cell line as a gift from Robert Molday, Ophthalmology and Visual Sciences, Centre for Macular Research, University of British Columbia, Vancouver, British Columbia, Canada[41]. Mouse monoclonal antibodies against the HA and FLAG tags were purchased from MBL (M180-3) and Sigma (F3165). The Alexa Fluor 488-conjugated Lectin PNA from *Arachis hypogaea* (peanut) was purchased from Thermo Fisher Scientific (L21409). The mouse monoclonal antibody against zebrafish Dcst2 was generated by the Max Perutz Labs Monoclonal Antibody Facility. Recombinant zebrafish Dcst2 (574-709), generated by VBCF Protein Technologies, served as the antigen. Horseradish peroxidase (HRP)-conjugated goat anti-mouse immunoglobulins (IgGs) (115-036-062) and HRP-conjugated goat anti-rat IgGs (112-035-167) were purchased from Jackson ImmunoResearch Laboratories. Fluorophore-conjugated secondary antibodies, goat anti-mouse IgG Alexa Fluor 488 (A11001), goat anti-mouse IgG Alexa Fluor 546 (A11018), goat anti-mouse IgG Alexa Fluor 594 (A11005), and goat anti-rat IgG Alexa Fluor 488 (A11006) were purchased from Thermo Fisher Scientific.

Mouse sperm fusion assay.

The fusion assay was performed as described previously[11]. To visualize IZUMO1 distribution in spermatozoa, spermatozoa after incubation of 2.5 hours in TYH drops were then incubated with the IZUMO1 monoclonal antibody (KS64-125, 1:100) for 30 minutes. Then, the spermatozoa were incubated with ZP-free eggs in TYH drops with the mixture of IZUMO1 monoclonal antibody (KS64-125, 1:100) and goat anti-rat IgG Alexa Fluor 488 (1:200) for 30 minutes. Then, the eggs were gently washed with a 1:1 mixture of TYH and FHM medium three times, and then fixed with 0.2% PFA. After washing again, IZUMO1 localization was observed under a fluorescence microscope (BZ-X700, Keyence).

HEK293T-oocyte binding assay.

Mouse *Dcst1* ORF-3xFLAG, mouse *Dcst2* ORF-3xHA, mouse *Izumo1* ORF-1D4 with a Kozak sequence (gccgcc) and a rabbit polyadenylation [poly (A)] signal were inserted under the CAG promoter. These plasmids (0.67 μg/each, total 2 μg) were transfected into HEK293T cells using the calcium phosphate-DNA coprecipitation method[42]. After 2 days of transfection, these cells were resuspended in PBS containing 10 mM (ethylenedinitrilo)tetraacetic acid. After centrifugation, the cells were washed with PBS, and then incubated with ZP-free eggs. After 30 minutes and then more than 6 hours of incubation, the attached and fused cell numbers were counted under a fluorescence

391 microscope (BZ-X700, Keyence) and an inverted microscope with relief phase contrast
392 (IX73, Olympus). Proteins were extracted from the remaining HEK293T cells with a
393 lysis buffer containing Triton-X 100 [50 mM NaCl, 10 mM Tris·HCl, 1% (vol/vol)
394 Triton-X 100 (Sigma Aldrich), pH 7.5] containing 1% (vol/vol) protease inhibitor
395 mixture, and then used for western blotting and co-IP.
396
397 **Co-IP.**
398 Protein extracts [1 mg (TGC), 95~105 μg (spermatozoa), and 200 μg (HEK293T)] were
399 incubated with anti-HA antibody coated Dynabeads Protein G for immunoprecipitation
400 (10009D, Thermo Fisher Scientific) for 1 hour at 4°C. After washing with a buffer (50
401 mM Tris-HCl, 150 mM NaCl, 0.1% Triton X-100, and 10% Glycerol, pH7.5), protein
402 complexes were eluted with SDS sample buffer containing β-mercaptoethanol (for
403 western blotting).
404
405 **Western blotting.**
406 Before SDS-PAGE, samples were mixed with sample buffer containing β-
407 mercaptoethanol[33], and boiled at 98°C for 5 minutes. For mouse samples, the
408 polyvinylidene difluoride (PVDF) membrane was treated with Tris-buffered saline
409 (TBS)-0.1% Tween20 (Nacalai Tesque) containing 10% skim milk (Becton Dickinson
410 and Company) for 1 hour, followed by the primary antibody [IZUMO1, SLC2A3, HA,
411 and FLAG (1:1,000), 1D4 (1:5,000)] for 3 hours or overnight. After washing with
412 TBST, the membrane was treated with secondary antibodies (1:1,000). For zebrafish
413 samples, after wet transfer onto nitrocellulose, total protein was visualized by Ponceau
414 staining before blocking with 5% milk powder in TBST. The primary antibody [mouse
415 anti-zebrafish-Dcst2 (1:50 in blocking buffer)] was incubated overnight at 4°C. The
416 membrane was washed with TBST before secondary antibody incubation for 1 hour.
417 The HRP activity was visualized with ECL prime (BioRad) and Chemi-Lumi One Ultra
418 (Nacalai Tesque) (for mouse) or ChemiDoc (BioRad) (for zebrafish). Then, the total
419 proteins on the membrane were visualized with Coomassie Brilliant Blue (CBB)
420 (Nacalai Tesque).
421
422 **Immunocytochemistry.**
423 After 3 hour incubation of mouse spermatozoa in TYH drops, the spermatozoa were
424 washed with PBS. The spermatozoa suspended with PBS were smeared on a slide glass,
425 and then dried on a hotplate. The samples were fixed with 1% PFA, followed by
426 permeabilizing with Triton-X 100. The spermatozoa were blocked with 10% goat serum
427 (Gibco) for 1 hour, and then incubated with a mouse monoclonal antibody against HA
428 tag (1:100) for 3 hours or overnight. After washing with PBS containing 0.05%
429 (vol/vol) Tween 20, the samples were subjected to the mixture of a goat anti-mouse IgG
430 Alexa Fluor 546 (1:300) and Alexa Fluor 488-conjugated Lectin PNA (1:2,000) for 1
431 hour. After washing again, the samples were sealed with Immu-Mount (Thermo Fisher
432 Scientific) and then observed under a phase contrast microscope (BX-50, Olympus)
433 with fluorescence equipment.
434 Zebrafish spermatozoa were fixed with 3.7% formaldehyde immediately after collection
435 at 4°C for 20 minutes. Spermatozoa were brought onto a SuperFrost Ultra Plus slide
436 (Fisher Scientific) with a CytoSpin 4 (Thermo Fisher Scientific) at 1,000 rpm for 5
437 minutes followed by permeabilization with ice-cold methanol for 5 minutes. The slide

was washed with PBS before blocking with 10% normal goat serum (Invitrogen) and 40 µg/mL BSA in PBST for 1 hour and then incubated with the mouse anti-zebrafish-Dcst2 antibody (1:25) overnight at 4°C. After washing with PBST, the slide was incubated with goat anti-mouse IgG Alexa Fluor 488 (1:100) for 2 hours before washing with PBST once more. After mounting using VECTASHIELD Antifade with DAPI (Vector Laboratories), spermatozoa were imaged with an Axio Imager.Z2 microscope (Zeiss) with an oil immersion 63x/1.4 Plan-Apochromat DIC objective.

Fertility assessment of adult zebrafish.

The evening prior to mating, the fish assessed for fertility and a TLAB *wt/wt* fish of the opposite sex were separated in breeding cages. The next morning, the fish were allowed to mate. Eggs were collected and kept at 28°C in E3 medium (5 mM NaCl, 0.17 mM KCl, 0.33 mM $CaCl_2$, 0.33 mM $MgSO_4$, 10^{-5}% Methylene Blue). The rate of fertilization was assessed approximately 3 hours post-laying. By this time, fertilized embryos have developed to ~1000-cell stage embryos, while unfertilized eggs resemble one-cell stage embryos. Direct comparisons were made between siblings of different genotypes (*wt/wt*, heterozygous mutant, homozygous mutant).

Collection of zebrafish eggs and spermatozoa.

Un-activated zebrafish eggs and spermatozoa were collected following standard procedures[43]. The evening prior to sperm collection, male and female zebrafish were separated in breeding cages (one male and one female per cage).

To collect mature, un-activated eggs, female zebrafish were anesthetized using 0.1% w/v tricaine (25x stock solution in dH2O, buffered to pH 7.0-7.5 with 1 M Tris pH 9.0). After being gently dried on a paper towel, the female was transferred to a dry petri dish, and eggs were carefully expelled from the female by applying mild pressure on the fish belly with a finger and stroking from anterior to posterior. The eggs were separated from the female using a small paintbrush, and the female was transferred back to the breeding cage filled with fish water for recovery.

To collect wt or mutant spermatozoa, male zebrafish were anesthetized using 0.1% tricaine. After being gently dried on a paper towel, the male fish was placed belly-up in a slit in a damp sponge under a stereomicroscope with a light source from above. Spermatozoa were collected into a glass capillary by mild suction while gentle pressure was applied to the fish's belly. Spermatozoa were stored in ice-cold Hank's saline (0.137 M NaCl, 5.4 mM KCl, 0.25 mM Na_2HPO_4, 1.3 mM $CaCl_2$, 1 mM $MgSO_4$, and 4.2 mM $NaHCO_3$). The male was transferred back to the breeding cage containing fish water for recovery. For western blot analysis, spermatozoa from 3 males was sedimented at 800 x *g* for 5 minutes. The supernatant was carefully replaced with 25 µL RIPA buffer [50 mM Tris-HCl (pH 7.5), 150 mM NaCl, 1 mM $MgCl_2$, 1% NP-40, 0.5% sodium deoxycholate, 1X complete protease inhibitor (Roche)] including 1% SDS and 1 U/µL benzonase (Merck). After 10 minutes of incubation at RT, the lysate was mixed and sonicated 3 times for 15 seconds of 0.5-second pulses at 80% amplitude (UP100H, Hielscher) interspersed by cooling on ice.

Zebrafish sperm approach and binding assays.

Imaging of zebrafish sperm approach

Spermatozoa were squeezed from 2–4 *wt/wt* male fish and kept in 150 µl Hank's saline containing 0.5 µM MitoTracker Deep Red FM (Molecular Probes) for >10 minutes on ice. Un-activated, mature eggs were obtained by squeezing a *wt/wt* female. To prevent activation, eggs were kept in sorting medium (Leibovitz's medium, 0.5 % BSA, pH 9.0) at RT. The eggs were kept in place using a petri dish with cone-shaped agarose molds (1.5% agarose in sorting medium) filled with sorting medium. Imaging was performed with a LSM800 Examiner Z1 upright system (Zeiss) with a 20x/1.0 Plan-Apochromat water dipping objective. Before sperm addition, sorting media was removed and 1 mL of E3 medium was carefully added close to the egg. Five to ten µl of the stained spermatozoa was added as close to the egg as possible during image acquisition. The resulting time-lapse movies were analyzed using FIJI.

Imaging and analysis of zebrafish sperm-egg binding

Spermatozoa was squeezed from 2–4 male fish and kept in 100 µL Hank's saline + 0.5 µM MitoTracker Deep Red FM on ice. Un-activated, mature eggs were squeezed from a *wt/wt* female fish and activated by addition of E3 medium. After 10 minutes, 1-2 eggs were manually dechorionated using forceps and transferred to a cone-shaped imaging dish with E3 medium. After focusing on the egg plasma membrane, the objective was briefly lifted to add 2-10 µL of stained spermatozoa (approximately 200,000-250,000 spermatozoa). Imaging was performed with a LSM800 Examiner Z1 upright system (Zeiss) using a 10x/0.3 Achroplan water dipping objective. Images were acquired until spermatozoa was no longer motile (5 minutes). To analyze sperm-egg binding, stably-bound spermatozoa were counted. Spermatozoa were counted as bound when they remained in the same position for at least 1 minute following a 90-second activation and approach time window. Data was plotted as number of spermatozoa bound per 100 µm of egg membrane.

Statistical analyses.

All values are shown as the mean ± SD of at least three independent experiments. Statistical analyses were performed using the two-tailed Student's t-test, Mann-Whitney U-test, and Steel-Dwass test after examining the normal distribution and variance. For zebrafish data, statistical analyses were performed in GraphPad Prism 7 software.

Data availability statement

RNA-seq data reported here (zebrafish adult tissues) were deposited at the Gene Expression Omnibus (GEO) and are available under GEO acquisition number GSE171906. The authors declare that the data that support the findings of this study are available from the corresponding authors upon request.

ACKNOWLEDGMENTS. We thank Natsuki Furuta, Eri Hosoyamada, Naoko Nagasawa, and the Biotechnology Research and Development (nonprofit organization) for excellent technical assistance; Carina Pribitzer for RNA-Seq library preparation for zebrafish adult tissues; Mirjam Binner, Anna Kogan and the animal facility personnel from the IMP for help with genotyping and taking excellent care of zebrafish; Karin Aumayr and her team of the biooptics facility at the Vienna BioCenter (VBC) for support with microscopy; the Protein Technology Facility and the Next Generation

Sequencing Facility at Vienna BioCenter Core Facilities (VBCF) for recombinant protein expression and zebrafish adult tissue RNA-Seq, respectively; the Max Perutz Labs Monoclonal Antibody Facility for generating anti-zebrafish Dcst2 antibodies; the entire Pauli lab for fruitful discussions, and Ms Ferheen Abbasi for critical reading of the manuscript. This work was supported by Ministry of Education, Culture, Sports, Science and Technology/Japan Society for the Promotion of Science KAKENHI (Grants-in-Aid for Scientific Research) Grants JP18K14612 and JP20H03172 to T.N., JP15H05573, JP16KK0180, and JP20KK0155 to Y.F., JP19J21619 to S.O., and JP19H05750, JP21H04753 to M.I.; Japan Agency for Medical Research and Development Grant JP21gm5010001 to M.I.; Takeda Science Foundation grants to T.N., Y.F. and M.I.; Mochida Memorial Foundation for Medical and Pharmaceutical Research grant to Y.F.; The Sumitomo Foundation Grant for Basic Science Research Projects to Y.F.; Senri Life Science Foundation grant to Y.F.; Intramural Research Fund (grants 30-2-5 and 31-6-3) for Cardiovascular Diseases of National Cerebral and Cardiovascular Center to Y.F.; Eunice Kennedy Shriver National Institute of Child Health and Human Development Grants R01HD088412 and P01HD087157 to M.I.; and the Bill & Melinda Gates Foundation (grant INV-001902 to M.I.). Work in the Pauli lab has been supported by the FWF START program (Y 1031-B28 to A.P.), the HFSP Career Development Award (CDA00066/2015 to A.P.), a HFSP Young Investigator Award to A.P., EMBO-YIP funds to A.P., a Boehringer Ingelheim Fonds (BIF) PhD fellowship to A.B., a HFSP postdoctoral fellowship to V.E.D., and a DOC PhD student fellowship from the Austrian Academy of Sciences to K.R.G. The IMP receives institutional funding from Boehringer Ingelheim and the Austrian Research Promotion Agency (Headquarter grant FFG-852936).

Author Contributions: T.N., A.P. and M.I. conceptualized research; T.N., A.B., Y.F., K.R.G., C.E., V.E.D., S.O., S.B., M.K., and K.P. performed research; T.N., A.B., Y.F., K.R.G., C.E., V.E.D., S.B., K.P., and M.I. analyzed data; L.E.C.Q. performed analysis of RNA-Seq data; and T.N. , A.B., K.R.G., V.E.D., A.P. and M.I. wrote the paper.

Conflict of Interest Statement: The authors declare no conflict of interest.

References

1 Bianchi, E., Doe, B., Goulding, D. & Wright, G. J. Juno is the egg Izumo receptor and is essential for mammalian fertilization. *Nature* **508**, 483-487 (2014).

2 Inoue, N., Ikawa, M., Isotani, A. & Okabe, M. The immunoglobulin superfamily protein Izumo is required for sperm to fuse with eggs. *Nature* **434**, 234-238 (2005).

3 Inoue, N. et al. Molecular dissection of IZUMO1, a sperm protein essential for sperm-egg fusion. *Development* **140**, 3221-3229 (2013).

4 Inoue, N., Hagihara, Y., Wright, D., Suzuki, T. & Wada, I. Oocyte-triggered dimerization of sperm IZUMO1 promotes sperm-egg fusion in mice. *Nat Commun* **6**, 8858 (2015).

5 Miyado, K. et al. Requirement of CD9 on the egg plasma membrane for fertilization. *Science* **287**, 321-324 (2000).

6 Le Naour, F., Rubinstein, E., Jasmin, C., Prenant, M. & Boucheix, C. Severely reduced female fertility in CD9-deficient mice. *Science* **287**, 319-321 (2000).

7 Kaji, K. *et al.* The gamete fusion process is defective in eggs of Cd9-deficient mice. *Nat Genet* **24**, 279-282 (2000).

8 Runge, K. E. *et al.* Oocyte CD9 is enriched on the microvillar membrane and required for normal microvillar shape and distribution. *Dev Biol* **304**, 317-325 (2007).

9 Lamas-Toranzo, I. *et al.* TMEM95 is a sperm membrane protein essential for mammalian fertilization. *Elife* **9**, e53913 (2020).

10 Fujihara, Y. *et al.* Spermatozoa lacking Fertilization Influencing Membrane Protein (FIMP) fail to fuse with oocytes in mice. *Proc Natl Acad Sci U S A* **117**, 9393-9400 (2020).

11 Noda, T. *et al.* Sperm proteins SOF1, TMEM95, and SPACA6 are required for sperm-oocyte fusion in mice. *Proc Natl Acad Sci U S A* **117**, 11493-11502 (2020).

12 Barbaux, S. *et al.* Sperm SPACA6 protein is required for mammalian Sperm-Egg Adhesion/Fusion. *Sci Rep* **10**, 5335 (2020).

13 Witwicka, H. *et al.* Studies of OC-STAMP in Osteoclast Fusion: A New Knockout Mouse Model, Rescue of Cell Fusion, and Transmembrane Topology. *PLoS One* **10**, e0128275 (2015).

14 Yagi, M. *et al.* DC-STAMP is essential for cell-cell fusion in osteoclasts and foreign body giant cells. *J Exp Med* **202**, 345-351 (2005).

15 Miyamoto, H. *et al.* Osteoclast stimulatory transmembrane protein and dendritic cell-specific transmembrane protein cooperatively modulate cell-cell fusion to form osteoclasts and foreign body giant cells. *J Bone Miner Res* **27**, 1289-1297 (2012).

16 Kodama, J. & Kaito, T. Osteoclast Multinucleation: Review of Current Literature. *Int J Mol Sci* **21** (2020).

17 Hartgers, F. C. *et al.* DC-STAMP, a novel multimembrane-spanning molecule preferentially expressed by dendritic cells. *Eur J Immunol* **30**, 3585-3590 (2000).

18 Eleveld-Trancikova, D. *et al.* The dendritic cell-derived protein DC-STAMP is highly conserved and localizes to the endoplasmic reticulum. *J Leukoc Biol* **77**, 337-343 (2005).

19 Sawatani, Y. *et al.* The role of DC-STAMP in maintenance of immune tolerance through regulation of dendritic cell function. *Int Immunol* **20**, 1259-1268 (2008).

20 Kim, M. H., Park, M., Baek, S. H., Kim, H. J. & Kim, S. H. Molecules and signaling pathways involved in the expression of OC-STAMP during osteoclastogenesis. *Amino Acids* **40**, 1447-1459 (2011).

21 Wilson, K. L., Fitch, K. R., Bafus, B. T. & Wakimoto, B. T. Sperm plasma membrane breakdown during Drosophila fertilization requires sneaky, an acrosomal membrane protein. *Development* **133**, 4871-4879 (2006).

22 Fitch, K. R. & Wakimoto, B. T. The paternal effect gene ms(3)sneaky is required for sperm activation and the initiation of embryogenesis in Drosophila melanogaster. *Dev Biol* **197**, 270-282 (1998).

23 Wilson, L. D. *et al.* The Caenorhabditis elegans spe-49 gene is required for fertilization and encodes a sperm-specific transmembrane protein homologous to SPE-42. *Mol Reprod Dev* **85**, 563-578 (2018).

24 Kroft, T. L., Gleason, E. J. & L'Hernault, S. W. The spe-42 gene is required for sperm-egg interactions during C. elegans fertilization and encodes a sperm-specific transmembrane protein. *Dev Biol* **286**, 169-181 (2005).

25 Wilson, L. D. *et al.* Fertilization in C. elegans requires an intact C-terminal RING finger in sperm protein SPE-42. *BMC Dev Biol* **11**, 10 (2011).

26 Hermann, B. P. *et al.* The Mammalian Spermatogenesis Single-Cell Transcriptome, from Spermatogonial Stem Cells to Spermatids. *Cell Rep* **25**, 1650-1667 e1658 (2018).

27 Yoshida, K. *et al.* A model of the acrosome reaction progression via the acrosomal membrane-anchored protein equatorin. *Reproduction* **139**, 533-544 (2010).

28 Satouh, Y., Inoue, N., Ikawa, M. & Okabe, M. Visualization of the moment of mouse sperm-egg fusion and dynamic localization of IZUMO1. *J Cell Sci* **125**, 4985-4990 (2012).

29 Palumbi, S. R. Speciation and the evolution of gamete recognition genes: pattern and process. *Heredity (Edinb)* **102**, 66-76 (2009).

30 Swanson, W. J. & Vacquier, V. D. The rapid evolution of reproductive proteins. *Nat Rev Genet* **3**, 137-144 (2002).

31 Herberg, S., Gert, K. R., Schleiffer, A. & Pauli, A. The Ly6/uPAR protein Bouncer is necessary and sufficient for species-specific fertilization. *Science* **361**, 1029-1033 (2018).

32 Yang, M. *et al.* Osteoclast stimulatory transmembrane protein (OC-STAMP), a novel protein induced by RANKL that promotes osteoclast differentiation. *J Cell Physiol* **215**, 497-505 (2008).

33 Noda, T., Shidara, O. & Harayama, H. Detection of the activator cAMP responsive element modulator (CREM) isoform ortholog proteins in porcine spermatids and sperm. *Theriogenology* **77**, 1360-1368 (2012).

34 Toyoda Y, Yokoyama. M., Hoshi T. Studies on the fertilization of mouse eggs in vitro. I. In vitro fertilization of eggs by fresh epididymal sperm. *Jap. J. Anim. Reprod.* **16**, 147-151 (1971).

35 Noda, T. *et al.* Seminal vesicle secretory protein 7, PATE4, is not required for sperm function but for copulatory plug formation to ensure fecunditydagger. *Biol Reprod* **100**, 1035-1045 (2019).

36 Goodson, S. G., Zhang, Z., Tsuruta, J. K., Wang, W. & O'Brien, D. A. Classification of mouse sperm motility patterns using an automated multiclass support vector machines model. *Biol Reprod* **84**, 1207-1215 (2011).

37 Matsumura, T. *et al.* Male mice, caged in the International Space Station for 35 days, sire healthy offspring. *Sci Rep* **9**, 13733 (2019).

38 Tokuhiro, K., Ikawa, M., Benham, A. M. & Okabe, M. Protein disulfide isomerase homolog PDILT is required for quality control of sperm membrane protein ADAM3 and male fertility [corrected]. *Proc Natl Acad Sci U S A* **109**, 3850-3855 (2012).

39 Fujihara, Y. *et al.* Expression of TEX101, regulated by ACE, is essential for the production of fertile mouse spermatozoa. *Proc Natl Acad Sci U S A* **110**, 8111-8116 (2013).

40 Ikawa, M. *et al.* Calsperin is a testis-specific chaperone required for sperm fertility. *J Biol Chem* **286**, 5639-5646 (2011).

41 Molday, L. L. & Molday, R. S. 1D4: a versatile epitope tag for the purification and characterization of expressed membrane and soluble proteins. *Methods Mol Biol* **1177**, 1-15 (2014).

42 Noda, T., Oji, A. & Ikawa, M. Genome Editing in Mouse Zygotes and Embryonic Stem Cells by Introducing SgRNA/Cas9 Expressing Plasmids. *Methods Mol Biol* **1630**, 67-80 (2017).

43 Westerfield, M. *The zebrafish book. A guide for the laboratory use of zebrafish (Danio rerio).* 4th edition (Univ. of Oregon Press, Eugene, 2000).

Figure legends

Figure 1. Male fertility of *Dcst1* and *Dcst2* mutant mice.

A) Multi-tissue gene expression analysis. *Dcst1* and *Dcst2* are abundantly expressed in the mouse testis. Beta actin (*Actb*) was used as the loading control. Br, brain; Th, thymus; Lu, lung; He, heart; Li, liver; Sp, spleen; Ki, kidney; Te, testis; Ov, ovary; Ut, uterus.

B) Median-normalized level of *Dcst1* and *Dcst2* mRNA expression during mouse spermatogenesis. *Dcst1* and *Dcst2* are strongly expressed in mid-round spermatids, corresponding to other fusion-related factors. Ud Sg, undifferentiated spermatogonia; A1-A2 Sg, A1-A2 differentiating spermatogonia; A3-B Sg, A3-A4-In-B differentiating spermatogonia; Prele Sc, preleptotene spermatocytes; Le/Zy Sc, leptotene/zygotene spermatocytes; Pa Sc, pachytene spermatocytes; Di/Se Sc, diplotene/secondary spermatocytes; Early St, early round spermatids; Mid St, mid round spermatids; Late St, late round spermatids; SC, Sertoli cells.

C) Male fecundity. Each male was caged with 2 *wt/wt* females for more than 1 month. $Dcst2^{d25/wt}$ and $Dcst2^{del/wt}$ males were used as the control (Ctrl). $Dcst1^{d1/d1}$, $Dcst2^{d25/d25}$, and $Dcst2^{del/del}$ males succeeded in mating [number of plugs: 19 (Ctrl), 17 ($Dcst1^{d1/d1}$), 42 ($Dcst2^{d25/d25}$), 24 ($Dcst2^{del/del}$)], but the females very rarely delivered pups [pups/plug: 9.0 ± 2.8 (Ctrl), 0.2 ± 0.2 ($Dcst1^{d1/d1}$), 0 ($Dcst2^{d25/d25}$), 0 ($Dcst2^{del/del}$)].

D) Egg observation after IVF. After 8 hours of incubation, pronuclei were observed in the control spermatozoa (asterisks). However, *Dcst1* KO and *Dcst2* KO spermatozoa accumulated in the perivitelline space (arrows).

E) Sperm fertilizing ability using cumulus-intact eggs *in vitro*. *Dcst1* KO and *Dcst2*

KO spermatozoa could not fertilize eggs [fertilization rates: 96.5 ± 7.1% (Ctrl, 231 eggs), 0% (*Dcst1*$^{d1/d1}$, 97 eggs), 0% (*Dcst2*$^{d25/d25}$, 197 eggs)].

F) Sperm fertilizing ability using ZP-free eggs *in vitro*. *Dcst1* KO and *Dcst2* KO spermatozoa rarely fertilized eggs [fertilization rates: 100% (Ctrl, 142 eggs), 0.8 ± 1.6% (*Dcst1*$^{d1/d1}$, 94 eggs), 0% (*Dcst2*$^{d25/d25}$, 88 eggs)].

Figure 2. Adhesion and fusion ability of *Dcst1* and *Dcst2* mutant spermatozoa to oocyte plasma membrane.

A and B) Binding ability. *Dcst1* KO and *Dcst2* KO spermatozoa could bind to the oolemma after 30 minutes of incubation (panel A). There is no significant difference in the sperm number bound to the oolemma (panel B) [binding spermatozoa/oocyte: 5.7 ± 2.0 (Ctrl, 113 eggs), 7.6 ± 4.7 (*Dcst1*$^{d1/d1}$, 89 eggs), 7.6 ± 3.5 (*Dcst2*$^{d25/d25}$, 89 eggs)]. N.S.: not significant ($p > 0.05$).

C) Detection of IZUMO1. The band signals of IZUMO1 in TGC and spermatozoa of *Dcst1*$^{d1/d1}$ and *Dcst2*$^{d25/d25}$ male mice were comparable to the control. SLC2A3, one of proteins in sperm tail, was used as the loading control.

D and E) Acrosome status of binding spermatozoa. Live spermatozoa bound to the oolemma were stained with the IZUMO1 antibody, and IZUMO1 only in the acrosome reacted (AR) spermatozoa was detected (panel D). There are no significant differences in the rates of AR spermatozoa (panel E) [AR spermatozoa/binding spermatozoa: 58.9 ± 17.9% (Ctrl), 80.5 ± 4.6% (*Dcst1*$^{d1/d1}$), 63.5 ± 6.5% (*Dcst2*$^{d25/d25}$)]. N.S.: not significant ($p = 0.13$).

F and G) Fusion ability. The ZP-free eggs pre-stained Hoechst 33342 were used for sperm-egg fusion assay. Hoechst 33342 signal transferred to control sperm heads, indicating that spermatozoa fused with eggs (panel F, arrow). However, *Dcst1* KO and *Dcst2* KO spermatozoa barely fused with eggs [fused spermatozoa/egg: 1.52 ± 0.35 (Ctrl, 113 eggs), 0.04 ± 0.05 (*Dcst1*$^{d1/d1}$, 73 eggs), 0 (*Dcst2*$^{d25/d25}$, 73 eggs)].

Figure 3. Detection of DCST1/2 in TGC and spermatozoa and interaction of DCST1/2.

A) Rescue of male fertility. *Dcst1*$^{d1/d1}$ males with *Dcst1*-3xHA Tg insertion and *Dcst2*$^{d25/d25}$ males with *Dcst2*-3xHA Tg insertion were generated (**Figure S6**), and their fertility was rescued [number of plugs: 17 (*Dcst1*$^{d1/d1}$), 25 (*Dcst1*$^{d1/d1}$;Tg), 42 (*Dcst2*$^{d25/d25}$), 15 (*Dcst2*$^{d25/d25}$;Tg)]. The fecundity data in *Dcst1*$^{d1/d1}$ and *Dcst2*$^{d25/d25}$ males is replicated from **Figure 1C**.

B) Detection of DCST1 and DCST2 in TGC and spermatozoa. The protein extract of TGC (100 μg) and spermatozoa (6.6x10^6 spermatozoa) was used for SDS-PAGE. The HA-tagged DCST1 and HA-tagged DCST2 were detected in TGC and spermatozoa. Total proteins in the membrane were visualized by CBB staining. Triangle marks show the expected molecular size of DCST1 (about 80 kDa) and DCST2 (about 77 kDa).

C) Localization of DCST2 in spermatozoa. The HA-tagged DCST2 was localized in the anterior acrosome before the acrosome reaction, and then translocated to the equatorial segment in acrosome-reacted spermatozoa (arrows). PNA was used as a marker for the acrosome reaction. The fluorescence in the sperm tail was non-specific.

D) Co-IP and western blotting of the interaction between IZUMO1 and DCST1/2. The TGC and sperm lysates from Ctrl, *Dcst1*;Tg, and *Dcst2*;Tg males were incubated with anti-HA tag antibody-conjugated magnetic beads, and then the eluted protein

752 complex was subjected to western blotting. The HA-tagged DCST1 was detected only
753 in the IP product from TGC, and the HA-tagged DCST2 was detected in the IP-product
754 from TGC and spermatozoa. IZUMO1 was not detected in the co-IP products. Red and
755 blue triangle marks show the expected molecular size of DCST1 (about 80 kDa) and
756 DCST2 (about 77 kDa), respectively.
757 **E) Interaction between DCST1 and DCST2 in HEK293T cells.** The protein lysate
758 collected from HEK cells overexpressing *Dcst1*-3xFLAG and *Dcst2*-3xHA was
759 incubated with anti-HA tag antibody-conjugated magnetic beads. The FLAG-tagged
760 DCST1 was detected in the eluted protein complex. ADAM1B, a sperm protein that
761 localizes to the sperm surface and is not involved in sperm-egg fusion, was used for
762 negative control.
763
764 **Figure 4. Binding assay between ZP-free eggs and HEK293T cells overexpressing**
765 ***Dcst1/2*.**
766 **A) Detection of DCST1/2 and IZUMO1.** FLAG-tagged DCST1, HA-tagged DCST2,
767 and 1D4-tagged IZUMO1 were detected in HEK293T cells overexpressing *Dcst1*-
768 3xFLAG, *Dcst2*-3xHA, and *Izumo1*-1D4.
769 **B and C) Observation of ZP-free eggs incubated with HEK293T cells**
770 **overexpressing *Dcst1/2* and *Izumo1*.** The HEK293T cells overexpressing *Dcst1* or
771 *Dcst2* did not attach to the oocyte membrane. Even when the HEK cells overexpressing
772 *Dcst1/2* were used for the assay, these cells failed to bind to ZP-free eggs. The
773 HEK293T cells overexpressing *Dcst1/2* and *Izumo1* could bind to the oocyte membrane
774 but could not fuse with an egg. N.S.: not significant ($p = 0.28$).
775
776 **Figure 5: *Dcst1* and *dcst2* are essential for male fertility in zebrafish.**
777 **A) *Dcst1* and *dcst2* mutant zebrafish are male sterile.** Quantification of fertilization
778 rates as assessed by the number of embryos that progress beyond the one-cell stage. Left
779 three panels: Males of different genotypes (*wt/wt* sibling (+/+; white); heterozygote
780 sibling (+/-; light grey); homozygote sibling (-/-; dark grey)) were crossed to *wt/wt*
781 females; right panel: homozygous mutant females (-/-; dark grey) of the indicated
782 genotypes were crossed to *wt/wt* males. The number of individual clutches and the total
783 number of eggs per genotype are indicated. Data are means ± SD; adj. ****$p < 0.0001$
784 (Kruskal-Wallis test with Dunn's multiple-comparisons test); n. s., not significant.
785 **B) *Dcst1* and *dcst2* mutant spermatozoa are morphologically normal.**
786 Representative differential interference contrast images of spermatozoa from *wt/wt*,
787 *dcst1*$^{-/-}$, *dcst2*$^{-/-}$, and *dcst1/2*$^{-/-}$ fish. Scale bar: 15 µm.
788 **C) Dcst2 localizes to the sperm head.** Immunofluorescent detection of Dcst2 protein
789 (cyan) in permeabilized zebrafish wt (top) or *dcst2*$^{-/-}$ (bottom) spermatozoa using an
790 antibody recognizing the RING-finger domain of zebrafish Dcst2. A counterstain with
791 DAPI (blue) detects the sperm DNA in the nucleus. Scale bar: 10 µm.
792 **D) *Dcst2* mutant spermatozoa are motile and reach the micropyle.** Images from a
793 time-lapse movie of *dcst2*$^{-/-}$ spermatozoa added to wt eggs. Spermatozoa (magenta)
794 were labelled with MitoTracker and added to non-activated eggs. Spermatozoa and eggs
795 were activated by addition of water just before the start of the movie. The micropyle
796 (white arrow), a preformed funnel in the egg coat through which the spermatozoa reach
797 the oolemma, is outlined with a dashed white line in the insets. Left image (36 seconds
798 after activation and sperm addition): no spermatozoon has entered the micropylar area.

Right image (70 seconds after activation and sperm addition): spermatozoa can readily be detected within the micropylar area. Scale bar: 75 µm.

E-F) *Dcst2* mutant spermatozoa are defective in stable binding to wt eggs. Images from a time-lapse movie of wt (left) or *dcst2*$^{-/-}$ (right) spermatozoa added to activated and dechorionated wt eggs. Spermatozoa (magenta) were labelled with MitoTracker and activated at the time of addition to the eggs. Wt spermatozoa show clear binding to the surface of the egg (inset), while *dcst2*$^{-/-}$ spermatozoa are unable to stably bind to the oolemma (E). Binding of spermatozoa was assessed by quantifying the number of stably-bound spermatozoa in a 1-min. time window (F). Scale bar: 100 µm. ****$p < 0.0001$ (Mann Whitney test).

Figure 1

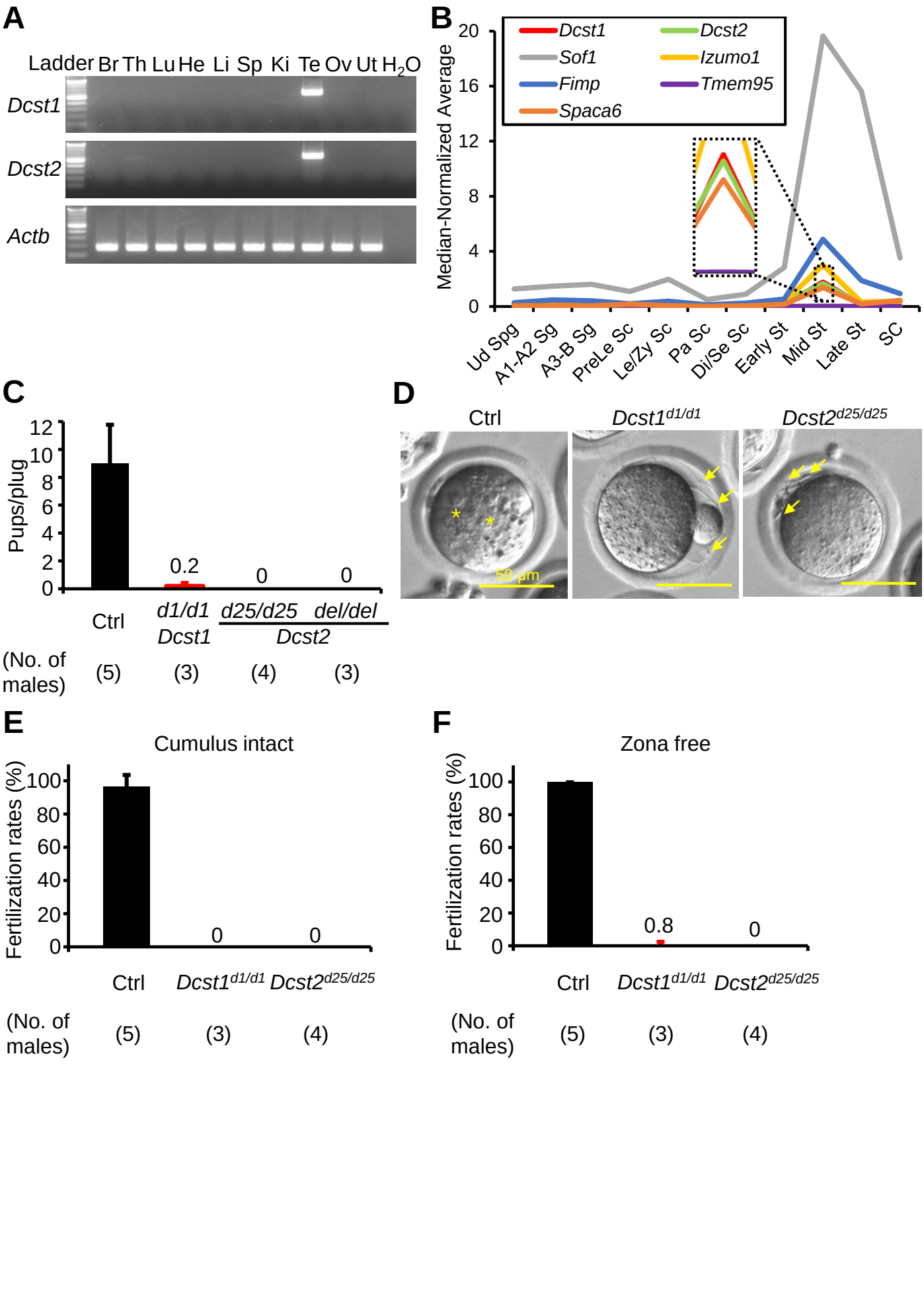

Figure 2

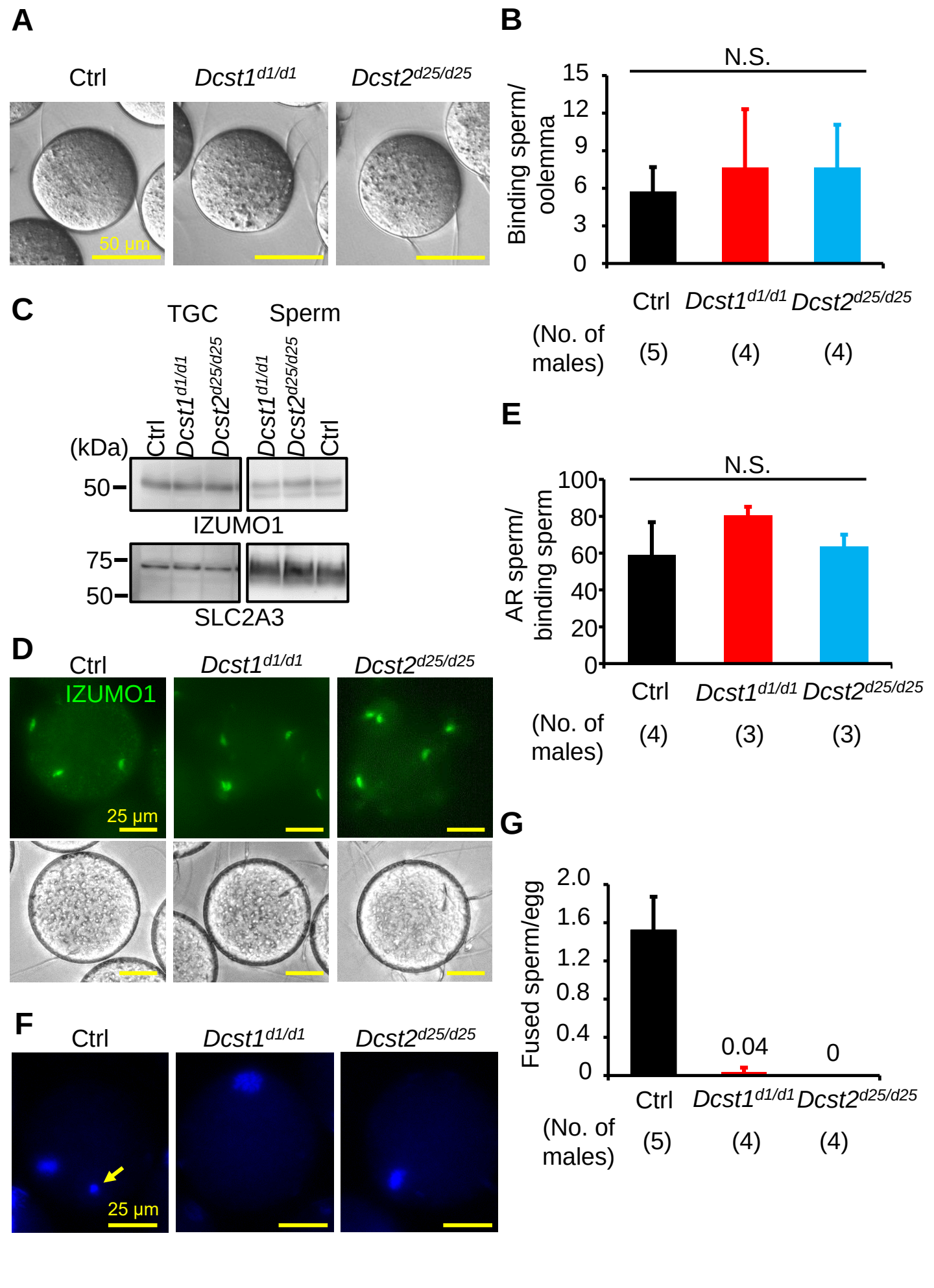

Figure 3

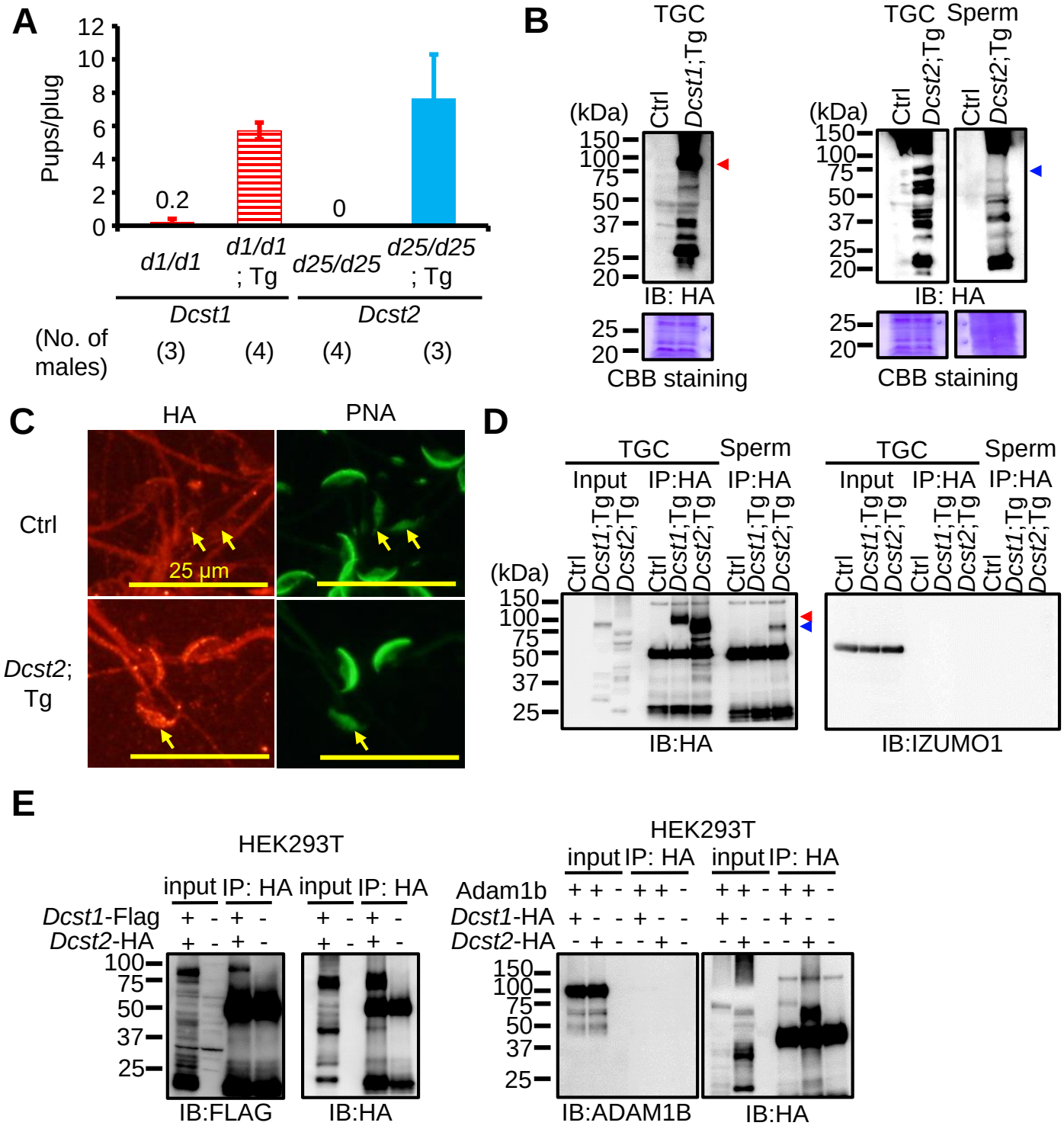

Figure 4

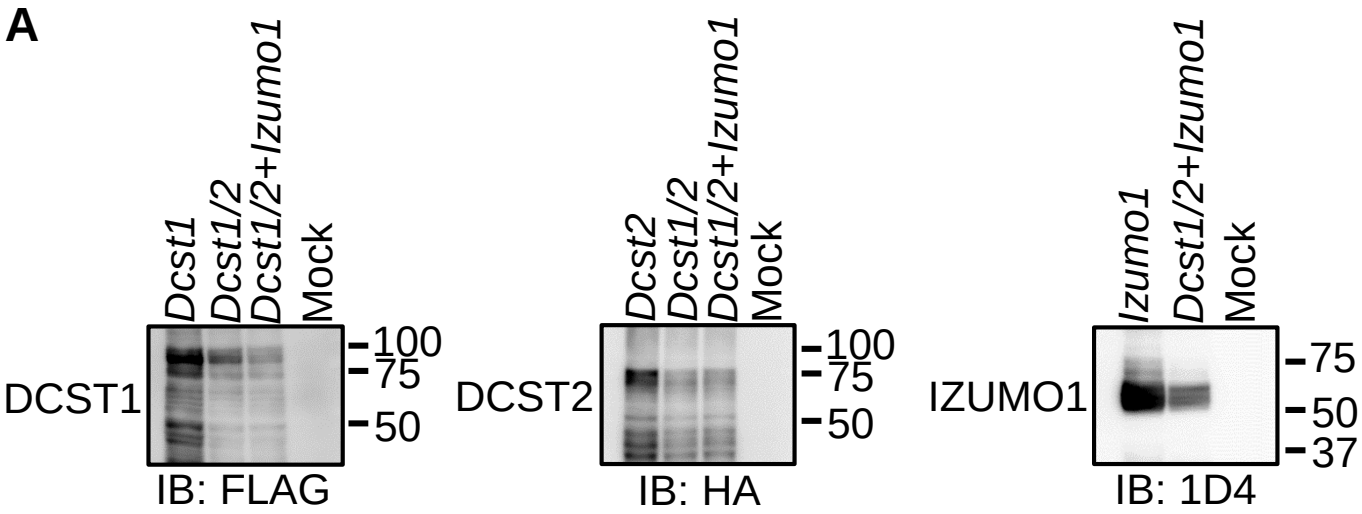

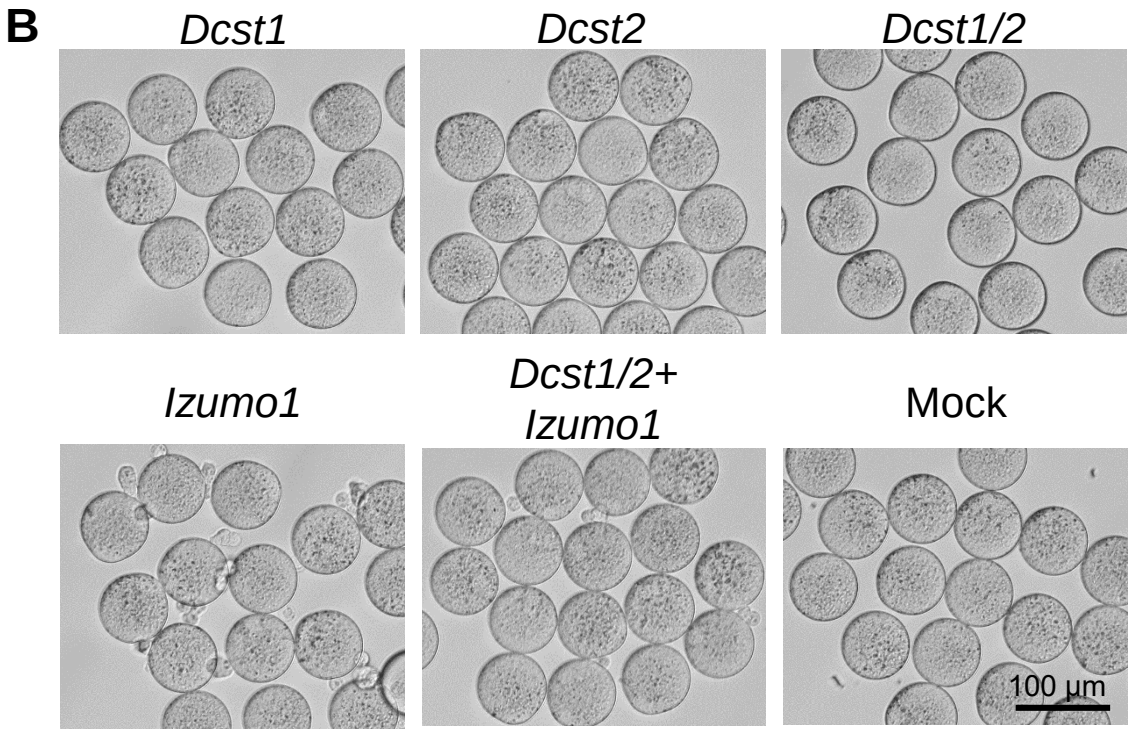

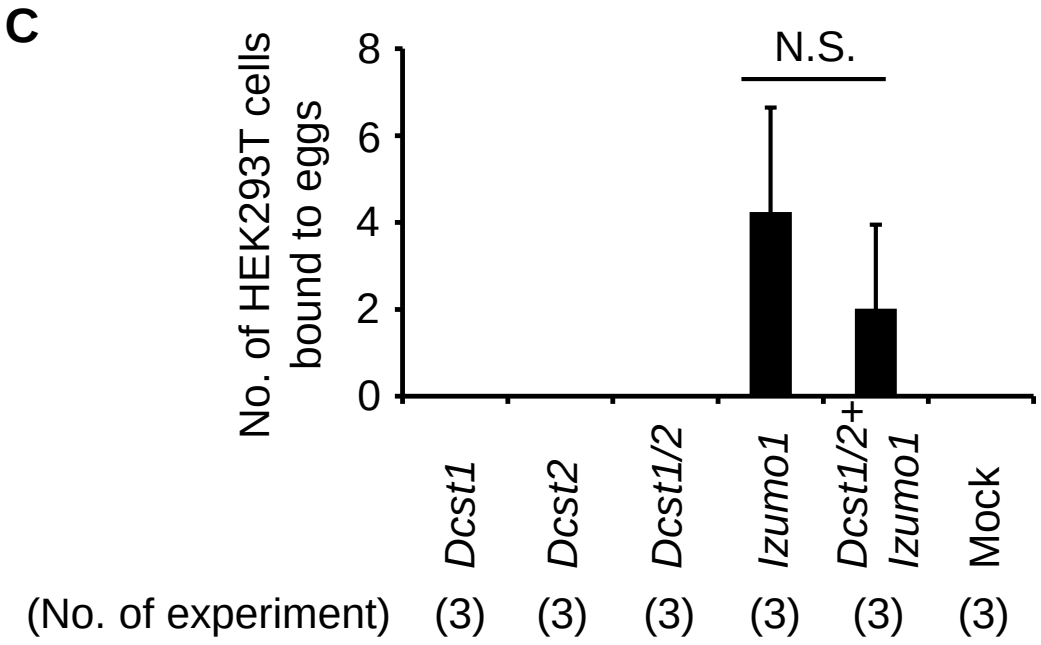

Figure 5